

RAPID REPORT

Novel approaches to determine contractile function of the isolated adult zebrafish ventricular cardiac myocyte

Alexey V. Dvornikov¹, Sukriti Dewan¹, Olga V. Alekhina¹, F. Bryan Pickett^{1,2} and Pieter P. de Tombe¹

¹Department of Cell and Molecular Physiology, Loyola University Chicago Stritch School of Medicine, Maywood, IL, USA

²Department of Biology, Loyola University Chicago, Chicago, IL, USA

Key points

- The zebrafish is emerging as an attractive cost-effective model for the study of structure–function relationships. However, cardiac contractile function in the zebrafish remains to be investigated.
- We applied novel approaches used to study contractile function at the cellular level in mammalian models to zebrafish. We found that contractile force regulation in the adult zebrafish shares many similarities with that in the mammalian myocardium as previously determined by others and ourselves, indicating that the zebrafish is an appropriate model system for the study of cardiac contractile biology.

Abstract The zebrafish (*Danio rerio*) has been used extensively in cardiovascular biology, but mainly in the study of heart development. The relative ease of its genetic manipulation may indicate the suitability of this species as a cost-effective model system for the study of cardiac contractile biology. However, whether the zebrafish heart is an appropriate model system for investigations pertaining to mammalian cardiac contractile structure–function relationships remains to be resolved. Myocytes were isolated from adult zebrafish hearts by enzymatic digestion, attached to carbon rods, and twitch force and intracellular Ca^{2+} were measured. We observed the modulation of twitch force, but not of intracellular Ca^{2+} , by both extracellular $[\text{Ca}^{2+}]$ and sarcomere length. In permeabilized cells/myofibrils, we found robust myofilament length-dependent activation. Moreover, modulation of myofilament activation–relaxation and force redevelopment kinetics by varied Ca^{2+} activation levels resembled that found previously in mammalian myofilaments. We conclude that the zebrafish is a valid model system for the study of cardiac contractile structure–function relationships.

(Received 3 January 2014; accepted after revision 27 February 2014; first published online 3 March 2014)

Corresponding author P. P. de Tombe: Department of Cell and Molecular Physiology, Stritch School of Medicine, Loyola University Chicago, 2160 South First Avenue, Maywood, IL 60153, USA. Email: pdetombe@lumc.edu

Abbreviations CL, cell length; EC_{50} , effective concentration 50%; FFT, fast Fourier transform; LDA, length-dependent activation; pCa , $-\lg [\text{Ca}^{2+}]$; pCa_{50} , effective pCa 50%; PKA, protein kinase A; SFR, slow force response; SL, sarcomere length.

Introduction

Over recent decades, the zebrafish (*Danio rerio*) has been used extensively in cardiovascular biology, albeit mainly in the study of heart development. Because of the ease of genetic manipulation in this species, the zebrafish has emerged as a promising and cost-effective model system

for the study of structure–function relationships (Bakkers, 2011; Becker *et al.* 2011; Ha *et al.* 2013). Despite this advantage, only a few studies have reported aspects of zebrafish cardiac electrophysiology (Nemtsas *et al.* 2010), Ca^{2+} homeostasis (Zhang *et al.* 2010; Bovo *et al.* 2013) or myofilament function (Iorga *et al.* 2011). Moreover,

whether adult zebrafish cardiac contractile physiology is comparable with that of the mammalian system has not been established, particularly in terms of twitch force responses to varied extracellular Ca^{2+} or sarcomere length (SL). Finally, methods to study mechanically loaded isolated twitching zebrafish myocardium have not been reported previously. Hence, the question of whether the zebrafish heart is an appropriate model system for investigations pertaining to mammalian cardiac contractile structure–function relationships remains to be answered.

Methods to measure single isolated cardiac myocyte twitch force have recently been improved substantially by the implementation of a cellular ‘glue’ (MyoTak) (Prosser *et al.* 2011). Here, we adopt this new methodology to study the contractile function of enzymatically isolated adult zebrafish ventricular myocytes. Two modes of contraction were studied: (i) electrically stimulated twitches in membrane-intact cells, and (ii) Ca^{2+} -activated contractions in Triton X-100 permeabilized cells. As in mammalian myocardium (ter Keurs *et al.* 1980; Kentish *et al.* 1986; de Tombe & ter Keurs, 1991), we observed the modulation of twitch force by both extracellular $[\text{Ca}^{2+}]$ and SL, as well as robust myofilament length-dependent activation (LDA). Moreover, myofilament activation–relaxation and force redevelopment kinetics regulation resembled those found previously in mammalian myofilaments (Poggesi *et al.* 2005; Iorga *et al.* 2011).

We conclude that the zebrafish is a valid and promising model system in which to study cardiac contractile structure–function relationships.

Methods

All experiments were performed according to institutional guidelines concerning the care and use of experimental animals. Zebrafish were locally bred using stock obtained from Aquatica Tropicals, Inc. (Plant City, FL, USA).

Isolation of ventricular myocytes

Single cardiac myocytes were isolated using an enzymatic digestion procedure as previously described (Bovo *et al.* 2013). Briefly, zebrafish were initially anaesthetized with tricaine (0.16 mg ml^{-1} in water at room temperature) and subsequently killed by immersion into ice-cold tricaine solution (5 min). Hearts were quickly excised and cannulated via the aorta to an ultrafine 34-gauge blunt needle and perfused for 30 min at 0.5 ml min^{-1} with a low Ca^{2+} fish Tyrode solution (Llach *et al.* 2011) also containing collagenase (0.2 mg ml^{-1} ; type 2; Worthington Biochemical Corp., Lakewood, NJ, USA) and trypsin (0.12 mg ml^{-1} ; type IX-S; Sigma-Aldrich Corp., St Louis, MO, USA). All experiments were performed at room temperature.

Membrane-intact isolated cell force measurement

The experimental set-up was similar to that described by Iribe *et al.* (2006) except for the method of cell attachment to the microprobes. In the present study, single isolated zebrafish cardiac ventricular cells were attached to carbon rods (Tsukuba Materials Information Laboratory Ltd, Tsukuba, Japan) using MyoTak glue (IonOptix LLC, Milton, MA, USA). The cells were paced via electrical field stimulation (1 Hz, 40V, 2 ms) and superfused with the fish Tyrode solution; $[\text{Ca}^{2+}]$ varied as indicated. Cell length (CL) was controlled and modulated by a Piezo translator (Physik Instrumente GmbH & Co. KG, Karlsruhe/Palmbach, Germany). In some experiments, the attached cell was stretched by 2.5–20.0% every 5 s (i.e. every fifth twitch) to assess length modulation of twitch force and intracellular $[\text{Ca}^{2+}]$.

Ca^{2+} transients

In some experiments, cells were loaded with $2 \mu\text{M}$ Indo1-AM (Molecular Probes, Inc., Eugene, OR, USA) for 15 min, followed by a 30 min washout. The excitation wavelength was 365 nm; fluorescence emission was measured at 405 nm and 485 nm. A variable rectangular aperture limited the emission field to the attached cell. Background fluorescence was subtracted from the raw signals in each channel. Note that motion artefacts were largely avoided by recording emitted fluorescence signals from the entire cell and by using a ratiometric calcium indicator.

Chemically permeabilized cells

Isolated ventricular muscle cells were permeabilized (skinned) at room temperature in standard relax skinned fibre solution with 1% Triton X-100 added for 5 min and mounted on a single myofibril set-up as previously described (de Tombe *et al.* 2007). These experiments were performed at 10°C .

Data processing and statistical analysis

Cell length (carbon rod edge detection), SL [fast Fourier transform (FFT)] and Indo-1 fluorescence signals were recorded and analysed using a combination of the IonOptix LLC system and custom-written LabView software for control of CL. Force data were normalized to cross-sectional area and expressed as mN mm^{-2} . Sigmoidal (modified Hill equation) and exponential relationships were fit to the data using non-linear regression routines (KaleidaGraph; Synergy Software, Reading, PA, USA). Group means were analysed by one-way ANOVA; linear relationships were analysed

by multiple regression, and a P -value of < 0.05 was considered indicative of statistical significance. Data are presented as the mean \pm S.E.M.

Results

Twitch force in electrically stimulated zebrafish isolated cardiac myocytes

We employed two carbon fibre probes with different stiffness properties as illustrated in Fig. 1A: one stiff probe

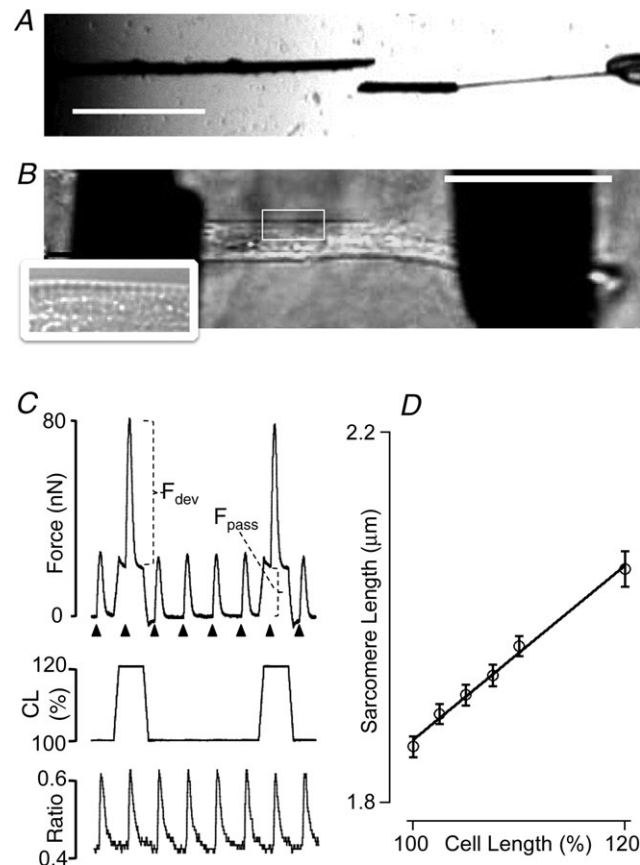


Figure 1. Membrane-intact mechanically loaded zebrafish myocytes

A, carbon rods coated with MyoTak glue were used to attach the myocytes: one rod was stiff (left; diameter 30 μm), and the other was compliant (right; diameter 10 μm). The latter was attached to a short stretch (30 μm) of the thicker probe, which increased attachment success. (Scale bar: 500 μm .) B, example of an attached membrane-intact enzymatically isolated myocyte. The inset shows a magnified region of the myocyte illustrating the appearance of sarcomere striations (observed in $\sim 30\%$ of cells). (Scale bar: 50 μm .) C, example of an original recording of twitch force (top) and Indo-1 fluorescence ratio (bottom). Cells were stimulated at 1 Hz (arrowheads; 40 V, 2 ms). Every fifth twitch, cells were stretched (here: 20%). Increased cell length (CL) induced an increase in passive force as well as active developed twitch force. D, relationship between video FFT-derived diastolic sarcomere length and overall CL ($n = 39$).

(left) was used as a cell stretcher, and one compliant probe (20–50 $\text{nN } \mu\text{m}^{-1}$; right) was used as a force transducer. The latter was glued to a short stretch of the thicker stiff probe ($\sim 30 \mu\text{m}$ diameter); we found that this approach greatly enhanced the successful forming of a firm attachment at this side of the cell. We used translation of the thick carbon fibre (cell stretch probe) to modulate CL. Determination of the displacement of the compliant probe by edge detection allowed us to calculate cell force development based on the measured stiffness of this probe. Figure 1B illustrates an isolated ventricular adult zebrafish myocyte attached using MyoTak glue to the two carbon rods. We were only able to measure SL in a subset of cells by FFT analysis of the microscope image, albeit mostly at the periphery of the cell (Fig. 1B, inset).

Figure 1C illustrates the impact of increased CL (middle) on twitch force (top) and cytosolic $[\text{Ca}^{2+}]$ (ratio; bottom). Cells were stretched every fifth twitch (here: 20%) 100 ms prior to electrical stimulation (arrows) inducing both increased passive force (F_{pass}) and active developed twitch force (F_{dev}). Neither diastolic $[\text{Ca}^{2+}]$ nor the amplitude of the calcium transient as reported by Indo-1 fluorescence were affected by cell stretch. Use of an intermittent stretch protocol allows for the assessment of instantaneous beat-to-beat SL modulation of contractile parameters while maintaining overall steady state contractility, an approach we have employed previously in the isolated multicellular cardiac trabecula preparation (ter Keurs *et al.* 1980; Kentish *et al.* 1986; de Tombe & ter Keurs, 1991).

Slack SL of the unattached zebrafish ventricular myocyte was, in the present experiments, equivalent to $\sim 1.8 \mu\text{m}$. Subsequent attachment required slight stretching of the cell to, on average, $1.86 \pm 0.01 \mu\text{m}$. Figure 1D illustrates a direct and linear relationship between CL and SL in the subset of cells that allowed for SL determination; on average a 20% increase in CL induced a $\sim 10\%$ increase in SL. Despite the use of MyoTak cell glue, cell stretches beyond 20%, in general, induced cell detachment, instability and/or cell death; hence, experiments reported here were limited to CL up to 120%. Moreover, reliable SL determination was possible only in a subset ($\sim 30\%$) of the zebrafish myocytes; hence, experiments reported here focused on overall CL instead.

Extracellular $[\text{Ca}^{2+}]$

Characteristically, mammalian myocardial contractility responds to increases in extracellular calcium ($[\text{Ca}^{2+}]_o$) in a dose-dependent manner, saturating at high $[\text{Ca}^{2+}]_o$ (Bers, 2008). That this is also the case in zebrafish myocardium is illustrated in Fig. 2. Twitch force (Fig. 2A) and the amplitude of the intracellular calcium transient (Fig. 2B) depended sigmoidally on $[\text{Ca}^{2+}]_o$. Moreover, as in mammalian myocardium, sensitivity to $[\text{Ca}^{2+}]_o$

for twitch force, as inversely indexed by the EC_{50} (Fig. 2A, inset), increased in proportion to CL. By contrast, the amplitude of the calcium transient was largely independent of CL. Figure 2C illustrates the impact of $[Ca^{2+}]_o$ on the twitch force–CL relationship. Again, as in mammalian myocardium (ter Keurs *et al.* 1980; Kentish *et al.* 1986; de Tombe & ter Keurs, 1991), the slope of this relationship increased in proportion to $[Ca^{2+}]_o$ (Fig. 2D).

Myofilament activation–relaxation kinetics

The amplitude of the calcium transient, in concert with the dynamic myofilament Ca^{2+} activation–relaxation

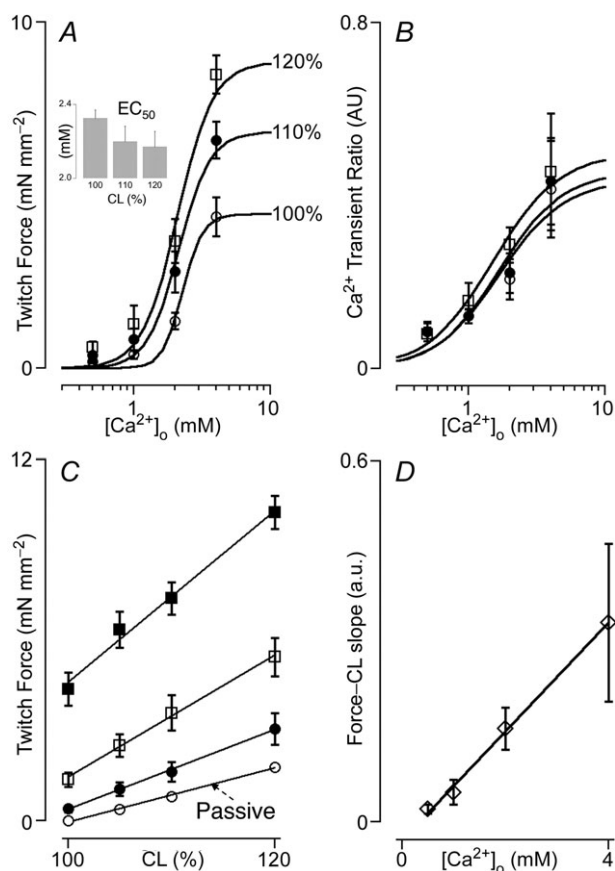


Figure 2. Impact of extracellular $[Ca^{2+}]$ and cell length on twitch force

A, twitch force–extracellular $[Ca^{2+}]$ relationships ($n = 10$). Increased cell length (CL) from baseline (open circles) to 10% (filled circles) and 20% (open squares) CL induced a leftward shift in the relationship, indicating enhanced sensitivity to $[Ca^{2+}]_o$; this is confirmed by the decrease in EC_{50} ($[Ca^{2+}]_o$ at 50% maximum twitch force; inset). B, intracellular $[Ca^{2+}]$, assayed by Indo-1 fluorescence ratio, increased as a function of $[Ca^{2+}]_o$, but was independent of CL ($n = 10$; symbols as in A). C, twitch force increased as a function of CL at $[Ca^{2+}]_o = 1$ mM (filled circles), 2 mM (open squares) and 4 mM (filled squares); passive force (open circles; arrow) also increased as a function of CL, but was not affected by $[Ca^{2+}]_o$. D, the twitch force–CL slope increased as a function of $[Ca^{2+}]_o$ ($n = 7$).

properties, determines twitch force and consequently the ventricular pressure waveform. The rapid solution-switching technique combined with an ultra-thin permeabilized single myofibril-sized preparation has been successfully applied to mammalian myocardium by ourselves and others to estimate myofilament Ca^{2+} -induced force dynamics (Poggesi *et al.* 2005; de Tombe *et al.* 2007). In general, mammalian single myofibrils are prepared by mechanical homogenization. The left panel of Fig. 3A illustrates a zebrafish myofibril obtained by this technique attached to two glass micro-tools. One of these (left) is mounted on a Piezo translation stage in order to allow for dynamic control of SL, and the other probe (right) is a black ink-coated calibrated cantilever that is used here as a force transducer. Because zebrafish ventricular myocytes are composed of only a few myofibrils, we also examined whether enzymatically isolated myocytes could be employed in this manner. The right panel of Fig. 3A illustrates a Triton X-100 permeabilized (skinned) isolated zebrafish myocyte similarly attached to two probes. In general, the dimensions of mechanically isolated myofibrils or skinned enzymatically isolated myocytes were comparable and, moreover, both preparations yielded close to identical activation–relaxation Ca^{2+} activation kinetics parameters. The left panel of Fig. 3B illustrates an original recording of a zebrafish skinned cardiomyocyte during an activation–relaxation cycle initiated by rapid (<5 ms) exposure to a saturating level of free $[Ca^{2+}]$ ($pCa = 4$) at both short (SL = 2.2 μm) and long (SL = 2.4 μm) SLs. As in the mammalian myofibril, force develops exponentially upon activation. During steady activation, a rapid release–restretch transient is imposed, a manoeuvre that forcibly dissociates most active cycling cross-bridges; the subsequent exponential redevelopment of force, termed k_{TR} , is an index of cross-bridge cycle kinetics (Brenner, 1988). As in the mammalian myofibril (Poggesi *et al.* 2005), force relaxation ensued in a biphasic manner upon removal of activator Ca^{2+} : a slow initial phase is followed by a rapid exponential phase (illustrated at an expanded time scale in Fig. 3B, right).

The rate of Ca^{2+} -induced force development (k_{ACT}) has been shown to depend on $[Ca^{2+}]$, accelerating at higher free $[Ca^{2+}]$ (Poggesi *et al.* 2005). That this is also the case in zebrafish myofibrils is illustrated in Fig. 3C (left panel), in which k_{ACT} is plotted as a function of pCa . Moreover, SL did not affect this relationship. k_{TR} , the rate of force redevelopment following the release–restretch manoeuvre, was similar to k_{ACT} and, likewise, was not affected by SL (data not shown).

The kinetics (k_{LIN}) and duration (t_{LIN}) of the slow phase of the biphasic relaxation of force induced by the rapid return to the relaxing solution ($pCa = 9$) were independent of the level of myofilament activation prior to relaxation (Fig. 3C, right). The kinetics of the

subsequent rapid exponential phase (k_{EXP}) were slightly, but significantly, faster following activation at higher levels of Ca^{2+} . SL affected none of the relaxation kinetics parameters (note that force levels at pCa of ~ 6 were too low to accurately assess the k_{EXP} parameter). Similar results have been reported previously for mammalian myofibril activation–relaxation parameters (Poggesi *et al.* 2005).

Myofilament length-dependent activation

A prominent characteristic of the mammalian cardiac sarcomere is increased sensitivity to activating Ca^{2+} ions for steady state force development upon an increase in SL. This phenomenon of myofilament LDA is believed to represent the cellular basis of the Frank–Starling law of the heart (Kentish *et al.* 1986; Konhilas *et al.* 2002). The molecular basis of LDA is still unknown and is subject to intense investigation (Mateja & de Tombe, 2012). As illustrated in Fig. 4, the adult zebrafish cardiac sarcomere displays robust LDA. Thus, as in mammalian myocardium, the steady state force–pCa relationship is shifted to the left and upward upon an increase in SL. Maximum Ca^{2+} saturated force was $\sim 10\%$ higher at the longer SL, and

myofilament Ca^{2+} sensitivity, as indexed by the pCa₅₀ parameter, increased by ~ 0.3 pCa units. By contrast, the level of cooperative activation was not affected by SL, which reflects a finding similar to that reported for mammalian myocardium (Dobesh *et al.* 2002).

Discussion

The aim of the present study was to determine whether the adult zebrafish constitutes a valid model system for the study of cardiac contractile structure–function relationships. Enzymatically isolated single cardiac zebrafish myocytes were studied in two modes of contraction: (i) intact electrically stimulated and mechanically loaded, and (ii) chemically permeabilized and Ca^{2+} -activated. We found that the regulation of contractile parameters in the zebrafish heart was similar to that found in the mammalian heart and conclude that the zebrafish is an appropriate model for the study of cardiac contractile biology.

The zebrafish is an attractive cardiac model system for several reasons: (i) it allows for relatively easy genetic manipulation (Bakkers, 2011); (ii) it is cost-effective; (iii)

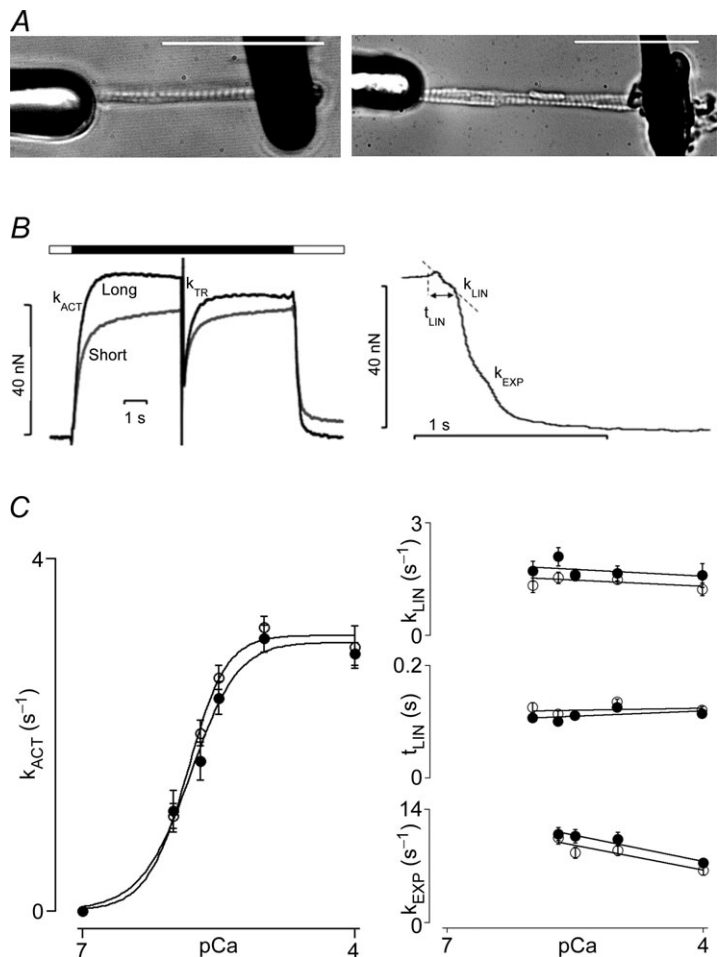


Figure 3. Myofilament activation–relaxation kinetics
 A, examples of a mechanically isolated myofibril (left panel; homogenization of an entire adult zebrafish heart) and a Triton X-100 permeabilized enzymatically isolated myocyte (right panel), both attached to glass microprobes. (Scale bars: 50 μm.) B, original recordings of myofibril force development at short (SL = 2.2 μm) and long (SL = 2.4 μm) sarcomere length (SL) during an activation–relaxation cycle at pCa = 9 (open bar) and pCa = 4 (filled bar); upon activation, force developed exponentially (k_{ACT}). At steady state force development, a rapid release–restretch manoeuvre was imposed to measure the rate of force redevelopment (k_{TR}); as illustrated in the right panel at an expanded time scale, relaxation of force ensued in a biphasic manner consisting of an initial slow linear phase (k_{LIN} , t_{LIN}), followed by a faster exponential phase (k_{EXP}). C, myofibril kinetic parameters as a function of activator Ca^{2+} (pCa) at SL = 2.2 μm (open circles) and SL = 2.4 μm (filled circles). The left panel shows the rate of force development k_{ACT} ; the right panel shows the rate (k_{LIN} ; top) and duration (t_{LIN} ; middle) of the slow linear phase, and the rate of the fast exponential phase (k_{EXP} ; bottom). k_{ACT} increased sigmoidally in proportion to activating Ca^{2+} , whereas relaxation dynamic parameters were largely independent of activating Ca^{2+} ; none of the activation–relaxation dynamic parameters were differentially affected by SL ($n = 20$).

the structure of critical domains of several sarcomeric proteins is conserved in the zebrafish (Fu *et al.* 2009), and (iv) the complete zebrafish genome has recently been sequenced, similarly to that of the mouse and human (Howe *et al.* 2013). Furthermore, the physiology of the adult zebrafish heart resembles that of the human heart in various respects. For example, both heart rate and action potential morphology are similar to those in the human (long plateau and action potential duration) (Brette *et al.* 2008), and indeed, the zebrafish has been used to model long QT syndrome (Arnaout *et al.* 2007). Likewise, we recently showed that the adult zebrafish is a useful model for the study of various aspects of calcium homeostasis in the heart, such as elementary Ca^{2+} spark generation and modulation of cellular Ca^{2+} homeostasis by adrenergic signalling (Bovo *et al.* 2013). Finally, the physiological body temperature of the zebrafish is close to room temperature (28°C) (Shiels & White,

2008), which represents a distinct practical advantage in experiments.

In this study, we focused on the regulation of contractile force, which is regulated by both extrinsic (contractile state) and intrinsic (SL) factors. The ultimate cellular mediator of contractile state is the magnitude of the intracellular Ca^{2+} transient. Indeed, we show here that: (i) there is a direct proportionality between extracellular Ca^{2+} and intracellular Ca^{2+} (Fig. 2B), and consequently twitch force (Fig. 2A) (Bers, 2008), and (ii) the magnitude of the intracellular Ca^{2+} transient is not affected by CL, at least not in the first twitch following cell stretch. Similar observations have been reported for isolated trout myocardium (Shiels *et al.* 2006) and, moreover, these characteristics have been well established in mammalian myocardium (Allen & Kurihara, 1979; Janssen & de Tombe, 1997; Bers, 2008). Likewise, robust increased intracellular Ca^{2+} transient amplitude upon application of the PKA agonist Forskolin, a response that was largely mediated by increased L-type Ca^{2+} channel function, has been demonstrated recently (Bovo *et al.* 2013). The persistent stretch of mammalian myocardium is accompanied by a slow increase in twitch force that develops over the course of several minutes, the so-called slow force response (SFR) (Cingolani *et al.* 2011). The precise mechanism underlying the SFR, caused by a gradual increase in intracellular Ca^{2+} upon stretch, is incompletely understood. Here, we found no evidence for SFR in zebrafish (data not shown), which is consistent with a recent report on trout myocardium (Patrick *et al.* 2011); absence of the SFR, therefore, may be a general feature of the teleost, and this would preclude the use of zebrafish myocardium for the direct study of SFR. However, the lack of an endogenous SFR may be useful in studies in which putative components of the mammalian SFR system are introduced by transgenesis. The shape of the force–SL relationship has been shown to be curvilinear and, moreover, the extent of this curvilinearity depends on extracellular $[\text{Ca}^{2+}]$ (ter Keurs *et al.* 1980; Kentish *et al.* 1986). Here, by contrast, we found close to linear relationships. However, it should be noted that our results are based on CL, not SL; therefore, neither the impact of cell attachment nor that of instrument compliance could be avoided altogether and this may have influenced the precise shape of the force–length relationship recorded.

Twitch force increased in proportion to stretch (Frank–Starling response) (Fig. 2). As in mammalian myocardium, the steepness of the force–length relationship increased in proportion to contractile state (ter Keurs *et al.* 1980; Kentish *et al.* 1986; de Tombe & ter Keurs, 1991). As the response to stretch occurred in the absence of a change in intracellular Ca^{2+} , these data indicate instead a change in myofilament Ca^{2+} sensitivity, which also explains the increased sensitivity to extracellular Ca^{2+} at the higher CL (Fig. 2A, inset). Indeed, examination of

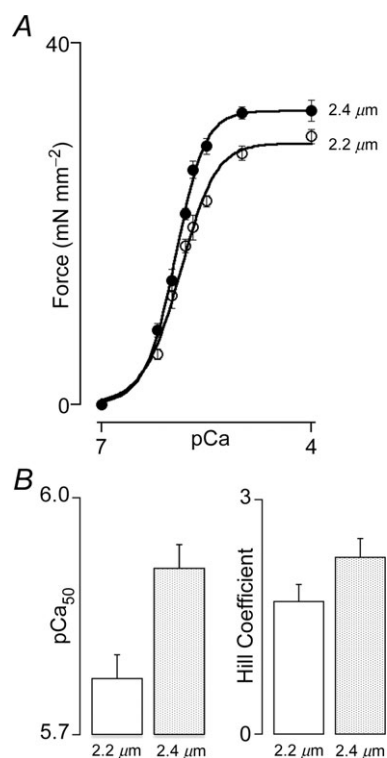


Figure 4. Myofilament length-dependent activation

A, steady state force development increased sigmoidally as a function of activating $[\text{Ca}^{2+}]$ at both short (SL = 2.2 μm ; open circles) and long (SL = 2.4 μm ; filled circles) sarcomere length (SL). Increased SL induced a leftward and upward shift of the relationship; maximum calcium saturated force was ~10% higher at the longer SL. B, increased SL was associated with increased myofilament calcium sensitivity (indexed by pCa₅₀, $-\log [\text{Ca}^{2+}]_i$) at 50% activation; $P < 0.05$), but no change in the level of cooperative activation (indexed by the Hill coefficient). These data indicate robust myofilament length-dependent activation in the adult zebrafish cardiac sarcomere ($n = 17$).

Ca^{2+} -activated force development in both permeabilized (skinned) zebrafish ventricular cells and skinned myofibrils revealed a robust myofilament length dependency, which was similar in magnitude to that found in the mammalian sarcomere (Mateja & de Tombe, 2012). Of note, a similar observation has been made in isolated trout myocardium (Patrick *et al.* 2010). Hence, myofilament LDA may be a general cardiac sarcomere property shared by both mammal and teleost, including the zebrafish. Of further note, the resting SL recorded in this study in zebrafish ($\sim 1.85 \mu\text{m}$) is virtually identical to that in all species studied to date (Shiels *et al.* 2006).

Twitch force is modulated by the magnitude of the Ca^{2+} transient and myofilament Ca^{2+} sensitivity, but also by the dynamic response of the sarcomere to activator Ca^{2+} . Here, we examined sarcomere Ca^{2+} activation–relaxation kinetic parameters by employing the single myofibril fast solution step technique (Poggesi *et al.* 2005). Our results confirm and expand on a previous study which reported similar mouse and zebrafish cardiac myofibril kinetics at saturating activating $[\text{Ca}^{2+}]$ (Iorga *et al.* 2011). Here, we found that the kinetics of force development (k_{ACT} and k_{TR}) strongly depended on activating $[\text{Ca}^{2+}]$, whereas relaxation parameters were largely independent of $[\text{Ca}^{2+}]$. Moreover, none of the parameters were affected by SL (Fig. 3). Overall, these characteristics are shared by the mammalian sarcomere (Poggesi *et al.* 2005). Of note, the enzymatically digested isolated zebrafish ventricular cell was composed of few myofibrils and is thus similar to the frog ventricular cell (Colomo *et al.* 1994). As a result, skinned cells behaved identically to myofibrils isolated by mechanical homogenization, the technique usually employed for mammalian myocardium (Poggesi *et al.* 2005). The advantage allowed by the single cell approach is the sequential study of intact twitching mechanics and permeabilized steady state and/or dynamic sarcomere function on the same preparation.

In summary, using novel approaches, we show that the zebrafish is an appropriate model for the study of cardiac contractile biology and this species may represent an attractive and cost-effective alternative for the study of cellular structure–function relationships.

References

- Allen DG & Kurihara S (1979). Calcium transients at different muscle lengths in rat ventricular muscle [proceedings]. *J Physiol* **292**, 68P–69P.
- Arnaout R, Ferrer T, Huisken J, Spitzer K, Stainier DY, Tristani-Firouzi M & Chi NC (2007). Zebrafish model for human long QT syndrome. *Proc Natl Acad Sci U S A* **104**, 11316–11321.
- Bakkers J (2011). Zebrafish as a model to study cardiac development and human cardiac disease. *Cardiovasc Res* **91**, 279–288.
- Becker JR, Deo RC, Werdich AA, Panakova D, Coy S & MacRae CA (2011). Human cardiomyopathy mutations induce myocyte hyperplasia and activate hypertrophic pathways during cardiogenesis in zebrafish. *Dis Model Mech* **4**, 400–410.
- Bers DM (2008). Calcium cycling and signalling in cardiac myocytes. *Annu Rev Physiol* **70**, 23–49.
- Bovo E, Dvornikov AV, Mazurek SR, de Tombe PP & Zima AV (2013). Mechanisms of Ca^{2+} handling in zebrafish ventricular myocytes. *Pflugers Arch* **465**, 1775–1784.
- Brenner B (1988). Effect of Ca^{2+} on cross-bridge turnover kinetics in skinned single rabbit psoas fibers: implications for regulation of muscle contraction. *Proc Natl Acad Sci USA* **85**, 3265–3269.
- Brette F, Luxan G, Cros C, Dixey H, Wilson C & Shiels HA (2008). Characterization of isolated ventricular myocytes from adult zebrafish (*Danio rerio*). *Biochem Biophys Res Commun* **374**, 143–146.
- Cingolani HE, Ennis IL, Aiello EA & Pérez NG (2011). Role of autocrine/paracrine mechanisms in response to myocardial strain. *Pflugers Arch* **462**, 29–38.
- Colomo F, Poggesi C & Tesi C (1994). Force responses to rapid length changes in single intact cells from frog heart. *J Physiol* **475**, 347–350.
- de Tombe PP & ter Keurs HE (1991). Sarcomere dynamics in cat cardiac trabeculae. *Circ Res* **68**, 588–596.
- de Tombe PP, Belus A, Piroddi N, Scellini B, Walker JS, Martin AF, Tesi C & Poggesi C (2007). Myofilament calcium sensitivity does not affect cross-bridge activation-relaxation kinetics. *Am J Physiol Regul Integr Comp Physiol* **292**, R1129–R1136.
- Dobesh DP, Konhilas JP & de Tombe PP (2002). Cooperative activation in cardiac muscle: impact of sarcomere length. *Am J Physiol Heart Circ Physiol* **282**, H1055–H1062.
- Fu C, Lee H & Tsai H (2009). The molecular structures and expression patterns of zebrafish troponin I genes. *Gene Expr Patterns* **9**, 348–356.
- Ha K, Buchan JG, Alvarado DM, McCall K, Vydyanath A, Luther PK, Goldsmith MI, Dobbs MB & Gurnett CA (2013). *MYBPC1* mutations impair skeletal muscle function in zebrafish models of arthrogryposis. *Hum Mol Genet* **22**, 4967–4977.
- Howe K, Clark MD, Torroja CF, Torrance J, Berthelot C, Muffato M, Collins JE, Humphray S, McLaren K, Matthews L, McLaren S, Sealy I, Caccamo M, Churcher C, Scott C, Barrett JC, Koch R, Rauch GJ, White S, Chow W, Kilian B, Quintais LT, Guerra-Assunção JA, Zhou Y, Gu Y, Yen J, Vogel JH, Eyre T, Redmond S, Banerjee R, Chi J, Fu B, Langley E, Maguire SF, Laird GK, Lloyd D, Kenyon E, Donaldson S, Sehra H, Almeida-King J, Loveland J, Trevanion S, Jones M, Quail M, Willey D, Hunt A, Burton J, Sims S, McLay K, Plumb B, Davis J, Clee C, Oliver K, Clark R, Riddle C, Elliot D, Threadgold G, Harden G, Ware D, Mortimore B, Kerry G, Heath P, Phillimore B, Tracey A, Corby N, Dunn M, Johnson C, Wood J, Clark S, Pelan S, Griffiths G, Smith M, Glithero R, Howden P, Barker N, Stevens C, Harley J, Holt K, Panagiotidis G, Lovell J, Beasley H, Henderson C, Gordon D, Auger K, Wright D, Collins J, Raisen C, Dyer L, Leung K, Robertson L, Ambridge K, Leongamornlert D, McGuire S, Gilderthorp R, Griffiths C, Manthavadi D, Nichol S,

- Barker G, Whitehead S, Kay M, Brown J, Murnane C, Gray E, Humphries M, Sycamore N, Barker D, Saunders D, Wallis J, Babbage A, Hammond S, Mashregi-Mohammadi M, Barr L, Martin S, Wray P, Ellington A, Matthews N, Ellwood M, Woodmansey R, Clark G, Cooper J, Tromans A, Grafham D, Skuce C, Pandian R, Andrews R, Harrison E, Kimberley A, Garnett J, Fosker N, Hall R, Garner P, Kelly D, Bird C, Palmer S, Gehring I, Berger A, Dooley CM, Ersan-Ürün Z, Eser C, Geiger H, Geisler M, Karotki L, Kirn A, Konantz J, Konantz M, Oberländer M, Rudolph-Geiger S, Teucke M, Osoegawa K, Zhu B, Rapp A, Widaa S, Langford C, Yang F, Carter NP, Harrow J, Ning Z, Herrero J, Searle SM, Enright A, Geisler R, Plasterk RH, Lee C, Westerfield M, de Jong PJ, Zon LI, Postlethwait JH, Nüsslein-Volhard C, Hubbard TJ, Roest Crollius H, Rogers J, Stemple DL, Begum S, Lloyd C, Lanz C, Raddatz G & Schuster SC (2013). The zebrafish reference genome sequence and its relationship to the human genome. *Nature* **496**, 498–503.
- Iorga B, Neacsu CD, Neiss WF, Wagener R, Paulsson M, Stehle R & Pfister G (2011). Micromechanical function of myofibrils isolated from skeletal and cardiac muscles of the zebrafish. *J Gen Physiol* **137**, 255–270.
- Iribe G, Helmes M & Kohl P (2006). Force–length relations in isolated intact cardiomyocytes subjected to dynamic changes in mechanical load. *Am J Physiol Heart Circ Physiol* **292**, H1487–H1497.
- Janssen PM & de Tombe PP (1997). Uncontrolled sarcomere shortening increases intracellular Ca^{2+} transient in rat cardiac trabeculae. *Am J Physiol Heart Circ Physiol* **272**, H1892–H1897.
- Kentish JC, ter Keurs HE, Ricciardi L, Bucx JJ & Noble MI (1986). Comparison between the sarcomere length–force relations of intact and skinned trabeculae from rat right ventricle. Influence of calcium concentrations on these relations. *Circ Res* **58**, 755–768.
- ter Keurs HE, Rijnsburger WH, van Heuningen R & Nagelsmit MJ (1980). Tension development and sarcomere length in rat cardiac trabeculae. Evidence of length-dependent activation. *Circ Res* **46**, 703–714.
- Konhilas J, Irving T & de Tombe P (2002). Frank–Starling law of the heart and the cellular mechanisms of length-dependent activation. *Pflugers Arch* **445**, 305–310.
- Llach A, Molina CE, Alvarez-Lacalle E, Tort L, Benítez R & Hove-Madsen L (2011). Detection, properties, and frequency of local calcium release from the sarcoplasmic reticulum in teleost cardiomyocytes. *PLoS One* **6**, e23708.
- Mateja R & de Tombe P (2012). Myofilament length-dependent activation develops within 5 ms in guinea-pig myocardium. *Biophys J* **103**, L13–L15.
- Nemtsas P, Wettwer E, Christ T, Weidinger G & Ravens U (2010). Adult zebrafish heart as a model for human heart? An electrophysiological study. *J Mol Cell Cardiol* **48**, 161–171.
- Patrick SM, Hoskins AC, Kentish JC, White E, Shiels HA & Cazorla O (2010). Enhanced length-dependent Ca^{2+} activation in fish cardiomyocytes permits a large operating range of sarcomere lengths. *J Mol Cell Cardiol* **48**, 917–924.
- Patrick SM, White E & Shiels HA (2011). Rainbow trout myocardium does not exhibit a slow inotropic response to stretch. *J Exp Biol* **214**, 1118–1122.
- Poggesi C, Tesi C & Stehle R (2005). Sarcomeric determinants of striated muscle relaxation kinetics. *Pflugers Arch* **449**, 505–517.
- Prosser BL, Ward CW & Lederer WJ (2011). X-ROS signaling: rapid mechano-chemo transduction in heart. *Science* **333**, 1440–1445.
- Shiels HA & White E (2008). The Frank–Starling mechanism in vertebrate cardiac myocytes. *J Exp Biol* **211**, 2005–2013.
- Shiels HA, White E, Shiels HA & Calaghan SC (2006). The cellular basis for enhanced volume-modulated cardiac output in fish hearts. *J Gen Physiol* **128**, 37–44.
- Zhang PC, Llach A, Sheng XY, Hove-Madsen L & Tibbits GF (2010). Calcium handling in zebrafish ventricular myocytes. *Am J Physiol Regul Integr Comp* **300**, R56–R66.

Additional information

Competing interests

None declared.

Author contributions

A.V.D., O.V.A. and P.P.d.T. designed and performed the experiments, analysed and interpreted the data, wrote the manuscript, and contributed to its discussion and review. S.D. and F.B.P. contributed to the design of the experiments and the review of the manuscript. All authors approved the final manuscript for submission.

Funding

This work was funded in part by National Institutes of Health awards (NIH HL62426 and HL75494) (P.P.d.T.), an American Heart Association postdoctoral fellowship grant (no. 14510047) (A.V.D.), and a President's Inter-Campus Research Initiative Award (P.P.d.T., F.B.P.).

Acknowledgements

None Declared.